XXXVI Ibero-Latin American Congress on Computational Methods in Engineering
CILAMCE
Rio de Janeiro, 22-25 Nov 2015

COMPUTATIONAL AND EXPERIMENTAL COMBUSTION ANALYSIS OF POROUS MEDIA IN A FIXED BED COMBUSTION REACTOR.

Alvino Oliveira Melo
alvino@ifma.edu.br
Emanuel Negrão Macêdo
enegrao@ufpa.br
Danielly Quaresma
danysq@gmail.com
Jose Antonio da Silva Souza
jass@ufpa.br
Alacid Neves
alacidneves@ufpa.br
Programa de Pós-Graduação em Engenharia de Recursos Naturais da Amazônia
Instituto de Tecnologia - Universidade Federal do Pará
Av. Augusto Corrêa - 01
Zip Code 001 66075 - 110 - Belém - Pará - Brazil

Márcio Ferreira Martins
marciofm@ct.ufes.br
Departamento de Engenharia Mecânica - Centro Tecnológico
Universidade Federal do Espírito Santo
Av. Fernando Ferrari, 514 - Goiabeiras
Zip Code 29075910, Vitória - ES - Brazil

Abstract. *Several experimental and theoretical studies of the combustion in porous media such as coal or wood particles in a fixed bed have been conducted in order to understand the phenomena that occur during the combustion process in porous media such as heat and mass transfer. To understand these processes of complex interpretations, a combustion reactor was developed and filled with a porous solid material, pellets, predominantly spherical in geometric shape, consisting of a mixture previously defined with a percentage of clay, fly ash and charcoal. The Data generated by the combustion reactor were recorded by " Paperless Recorder ". To validate the results a computational analysis was implemented by a computer program developed by the University of Toulouse. The results generated experimentally and numerically were plotted and analyzed.*

Keywords: *Computational combustion, Combustion reactor, Clay, Fly ash, Porous media*

1 INTRODUCTION

Porous medium mean a material that consist of a solid matrix with an interconnected void. Suppose that the solid matrix is either rigid, the usual situation, or it undergoes small deformation. The interconnectedness of the void or pores allows the flow of one or more fluids through the material. As examples of natural porous media can cite beach sand, sandstone, limestone, wood, and the human lung. (Bejan, 2006).

Several experimental and theoretical studies of the combustion of coal or wood particles in a fixed bed have been conducted in order to understand the phenomena that occur during the combustion process in porous media such as heat and mass transfer. However, the parameters that govern the combustion of solids in the bed, such as the effects of particle size, heat and mass transfer in porous media, and the interference between the solids reactions and gas phase, are not fully understood, (Kaviany,1995). To understand these processes of complex interpretations, a combustion reactor was developed and filled with a porous solid material, pellets, predominantly spherical in geometric shape, consisting of a mixture previously defined with a percentage of clay, from the banks of the Guamá River, fly ash from the steel industries of Pará-Brazil and charcoal.

The fuel used in the combustion reaction was charcoal, crushed in a disc mill in order to control the grain size. In this work were studied parameters such as the rate of supply of air, the influence of the size of the fuel particles (charcoal) and pellets (clay, charcoal and fly ash) during the combustion reaction. The method of volume averaging it's used to show equations that express the conservation of energy principle to porous medium. Data acquisition was taken by "Paperless Recorder PHL" properly attached to the thermocouples axially distributed throughout the combustion reactor. To validate the results a computational analysis was implemented by a computer program developed by the University of Toulouse. The results generated experimentally and numerically were plotted and analyzed.

2 DESCRIPTION AND EXPERIMENT SET UP

The experiment consists of a fixed bed reactor shown in Fig. (1a), it is based in a work developed in the Université de Tolouse by Martins (2008) . The fixed bed reactor is a cylinder made of carbon steel with a thickness of 1/8" with 158 mm internal diameter, 700 mm height and 164mm of external diameter shown in Fig. (1b). For getting one-dimensional propagation of the combustion front, walls of the reactor are insulated by an insulation layer of rock wool fiber with 30mm thickness. By means of this insulation radial losses are minimized and propagation on the reactor axis can be considered one-dimensional. Seven type K thermocouples are distributed throughout the reactor, keeping appropriate distances, shown in Fig. (1a) and Fig. (1b). Figure (1a), shows the reactor in situ. The data taken by "Paperless Recorder PHL" shown in Fig. (1c), were plotted and analyzed.

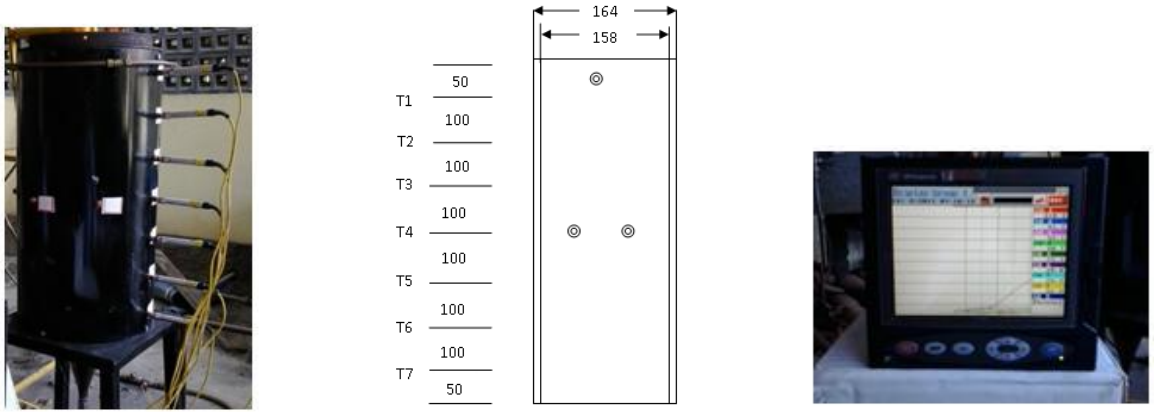

(a) (b) (c)

Figure 1 - (a) Combustion reactor in situ; (b) Reactor schematic draw; (c) Paperless Recorder

3 EXPERIMENTAL PROCEDURE

3.1 Pellets Production and Combustion Reaction Procedures

The production of the pellets are described in the six steps following:
i) Drying the coal and clay in a electric kiln at a temperature of 105°C;
ii) Crushing the coal in a disc mill;
iii) Grind coal and clay for 30 minutes in a ball mill;
iv) Homogenization of the coal, clay and fly ash in the ball mill during one hour;
v) Production of aggregates in a cement mixer;
vi) The aggregates (pellets) produced were removed from the mixer and heated in a electric kiln at 105°C for a period of 24 hours. The pellets were manufactured with 40% clay, 30% fly ash and 30% charcoal powder.

The fixed bed reactor was filled with 80% of coal milled with size suitably selected with sieves and 20% pellets until a height of 700 mm (completely filled). The fuel (coal milled) was slightly compressed and the procedure was adopted for the different tests. The ignition of the solid fuel (coal milled) begins with an external flame of a burner, using butane gas as a fuel, uniformly distributed across the surface of the fuel as shown in Fig. 2, to make the process homogeneous. After completing the process of ignition, start the self sustenance of the flame propagation. The time for ignition of the fuel and the self sustenance flame was about 6 minutes when the thermocouple 1, placed at a distance of 50mm from the top of the reactor, accused a temperature of approximately 700°C, then cut the fuel (butane gas) to the burner and the combustion reaction progressed self sustained. The burner was placed at a distance of about 13mm from the top of the reactor.

Figure 2- Combustion Ignition of the solid fuel in the combustion cell

The process variables are the velocity of the oxidant forced flow, the diameter of the pellets and the coal particle size. Temperatures are recorded as a function of time by the seven thermocouples distributed axially along the reactor and properly connected to the data logger (Paperless Recorder). The propagation of the reaction front is determined by the time taken for the reaction cross two consecutive thermocouples. The arrival of the reaction front in a thermocouple is determined by a sudden increase in temperature. Only thermocouples placed in the center line of the fuel bed is used to calculate the speed of propagation of the flame front, (X. Zhou, 1995).

4 NUMERICAL MODEL

Nomenclature

t	Time, s
x	Position in x-axis, m
R	Perfect gas constant, $J.K^{-1}.mol^{-1}$
P	Pressure, Pa
κ	Porous media permeability, m^2
Q	Heat reaction rate, $J.s^{-1}.m^{-3}$
M	Molar mass, $kg.mol^{-1}$
T	Temperature, K
$\vec{V}$	See page velocity, $m.s^{-1}$
v_g	Flow per unit area in Darcy law, $m.s^{-1}$
$\dot{R}$	Reaction rate, $kg.s^{-1}.m^{-3}$
C	Specific heat of the solid, $J.kg^{-1}.K^{-1}$
C_p	Specific heat at constant pressure, $J.kg^{-1}.K^{-1}$
D	Dispersion coefficient, $m^2.s^{-1}$
h	Thermal loss through walls, $J.s^{-1}.m^{-2}.K^{-1}$
Y	Mass fraction

Greek Symbols

∇	Gradient
$\nabla.$	Divergence
ε	Volume fraction
μ	Viscosity, $kg.s^{-1}.m^{-1}$
Γ	exchange coefficient, $J.s^{-1}.m^{-2}.K^{-1}$

ρ	Density, $kg.m^{-3}$
λ	Thermal conductivity, $J.m^{-1}.s^{-1}.K^{-1}$

Indices, exponents

*	Effective
f	fluid
s	Solid
k	Constituent k
g	Gas
k	{N_2, O_2, CO, CO_2, $CaCO_3$,fuel}
amb	Ambient

4.1 Principle of the Local Average Volume

A mathematical model that expresses the heat transfer in porous media is expressed considering the first law of thermodynamics. Consider that the medium is isotropic where radiative effects, viscous dissipation and the work done by pressure changes are negligible. It is assumed the hypothesis of local thermal equilibrium where $T_s = T_f = T$, is the temperature of the solid phase and fluid respectively. It is also assumed that the heat conduction in the solid and fluid phases occur simultaneously, so there is no net heat transfer from one phase to another. Considering the hypothesis above mentioned, the equations that express the conservation of energy principle to porous medium, taking in consideration the solid and fluid phases, can be written as:

$$\left(\rho C\right)_s \frac{\partial T_s}{\partial t} = \nabla.\left(\lambda_s \nabla T_s\right) + h_c\left(T_s - T_f\right) + \ddot{q}_s \tag{1}$$

$$\left(\rho C_p\right)_f \frac{\partial T_f}{\partial t}\left(\rho C_p\right)_f .\vec{V}.\nabla T_f = \nabla.\left(\lambda_f \nabla T_f\right) + h_c\left(T_f - T_s\right) + \ddot{q}_f \tag{2}$$

Using the principle of the local average volume Whitaker (1988), the equation for the solid phase can be written as below:

$$\left(1-\varepsilon\right)\left(\rho C\right)_s \frac{\partial \langle T_s \rangle}{\partial t} = \left(1-\varepsilon\right)\nabla.\left(\lambda_s \nabla \langle T_s \rangle\right) + \left(1-\varepsilon\right)\left[\langle \ddot{q}_s \rangle + h_c\left(\langle T_s \rangle - \langle T_f \rangle\right)\right] \tag{3}$$

and to fluid phase

$$\varepsilon\left(\rho C_p\right)_f \frac{\partial \langle T_f \rangle}{\partial t} + \varepsilon\left(\rho C_p\right)_f \vec{V}.\nabla \langle T_f \rangle = \varepsilon\nabla.\left(\lambda_f \nabla \langle T_f \rangle\right) + \varepsilon\left[\langle \ddot{q}_f \rangle + h_c\left(\langle T_f \rangle - \langle T_s \rangle\right)\right] \tag{4}$$

The subscripts s and f refer to the solid and fluid phases, respectively, C is the specific heat of the solid, C_P is the specific heat at constant pressure of the fluid, λ is the thermal conductivity, and $\ddot{q}$ [W/m^3] is the heat production per unit volume. Writing equations (3) and (4) it is assumed that the surface porosity is equal to the porosity ε. This is pertinent to the conduction terms. For example, $-\lambda_s \nabla \langle T_s \rangle$ is the conductive heat flux through the solid, and thus $\nabla.(\lambda_s \nabla \langle T_s \rangle)$ is the net rate of heat conduction into a unit volume of the solid. The Eq. (3) appears multiplied by the factor $(1-\varepsilon)$, which is the ratio of the cross-sectional area occupied by solid to the total cross-sectional area of the medium. The other two terms in Eq. (3) also contain the factor $(1-\varepsilon)$ because this is the ratio of volume occupied by solid to the total volume of the element. In Eq. (4) there also appears a convective term, due to the seepage velocity. Recognize that $\vec{V}.\nabla \langle T_f \rangle$ is the rate of change of temperature in the elemental volume due to the convection of fluid into it, so this, multiplied by $(\rho C_p)_f$, must be the rate of change of thermal energy, per unit volume of fluid, due to the convection. Considering an existence of a perfect contact between the solid phase and the fluid phase, it can consider the possibility of local thermal equilibrium between the phases, then:

$$\langle T_f \rangle = \langle T_s \rangle = \langle T \rangle \tag{5}$$

Adding the equations (3) e (4) and using the equation (5), it gets:

$$(\rho C_p)_{eff} \frac{\partial \langle T \rangle}{\partial t} + \varepsilon (\rho C_p)_f \vec{V}.\nabla \langle T \rangle = \nabla.(\lambda_{eff} \nabla \langle T \rangle) + \langle \ddot{q}_{eff} \rangle \tag{6}$$

where,

$$(\rho C_p)_{eff} = (1-\varepsilon)(\rho C)_s + \varepsilon (\rho C_p)_f \tag{7}$$

$$\lambda_{eff} = (1-\varepsilon)\lambda_s + \varepsilon \lambda_f \tag{8}$$

$$\langle \ddot{q}_{eff} \rangle = (1-\varepsilon)\langle \ddot{q}_s \rangle + \varepsilon \langle \ddot{q}_f \rangle \tag{9}$$

are, respectively, the overall heat capacity per unit volume, overall thermal conductivity, and overall heat production per unit volume of the medium.

4.2 One-Dimensional Numerical Model

The mathematical model used in this study was developed by the "Institut de Mecanique des Fluides of Toulouse" (IMFT), (Lapene, et al. 2008), To solve the equations of heat and mass transfer in reactive porous medium, in this model, It is used Darcy equation. Thermal local no equilibrium transport was allowed by the model, and treated with a two temperature model: one for the gas phase and another one for the solid phase. The chemical reactions considered are oxidation of fixed carbon and decarbonation reaction.

4.2.1 Mathematical Formulation

4.2.2 Simplifying hypotheses

1. The problem is one-dimensional

$$\nabla = \frac{\partial}{\partial x} \tag{10}$$

2. The porosity is constant in time and space

$$\frac{\partial \varepsilon_g}{\partial x} = \frac{\partial \varepsilon_s}{\partial x} = \frac{\partial \varepsilon_g}{\partial t} = \frac{\partial \varepsilon_s}{\partial t} = 0 \tag{11}$$

3. Considers the gas as ideal gas.

This hypothesis is considered because the pressure in the porous medium are values around to atmospheric pressure, then:

$$P = \rho_g \; r \, T, \;\; \text{where} \;\; r = \frac{R}{M_g} \tag{12}$$

4.2.3 Conservation Equations

In this work, taking into consideration Martins, (2008), where a heat and mass transport modeling was done in a porous reactive medium using a description on the scale of Darcy Local non equilibrium transport of heat was treated with a two field temperature model, one for the gas phase and one for the solid phase. The SiO_2 e de $CaCO_3$ could be triggered during the sintering of the pellets.

For generation of computer numerical data, it was took into consideration the reaction of carbonation which is covered by the program. Reactions, among others, which could occur during the sintering of the pellets:

1 - $Si + O_2 \rightarrow SiO_2$

2 - $CaO + CO_2 \rightarrow CaCO_3$

3 - $2Al(OH)_3 + \text{heat} \rightarrow Al_2O_3 + 3H_2O$

Phase composition

i) Solid phase: Pellets (clay, charcoal and fly ash); crushed charcoal used as fuel; inert matter (fly ash and clay).

ii) Fluid phase: gases N_2, O_2, CO, CO_2 .

Considering the assumptions mentioned, it writes the mass balance equations, energy and momentum as follow.

1) Mass Balance

- Continuity equation for gas phase

$$\varepsilon_g \frac{\partial \rho_g}{\partial t} + \frac{\partial}{\partial x}\left(\rho_g v_g\right) = \dot{R}_g \tag{13}$$

- Species transport

$$\varepsilon_g \frac{\partial \rho_g Y_k}{\partial t} + \frac{\partial}{\partial x}\left(\rho_g v_g Y_k\right) - \frac{\partial}{\partial x}\left(\rho_g D_k^* \frac{\partial Y_k}{\partial x}\right) = \dot{R}_{g,k} \tag{14}$$

2) Darcy Equation, neglecting gravity

$$v_g = -\frac{\kappa}{\mu_g}\frac{\partial P}{\partial x} \tag{15}$$

3) Energy Equations

- Gas phase energy balance

$$\varepsilon_g \left(\rho C_p\right)_g \frac{\partial T_g}{\partial t} + \left(\rho C_p\right)_g v_g \frac{\partial T_g}{\partial x} = \frac{\partial}{\partial x}\left(\lambda_g^* \frac{\partial T_g}{\partial x}\right) + \Gamma_{s,g}\left(T_g - T_s\right) + Q_g + h\left(T_{amb} - T_g\right) \tag{16}$$

- Solid phase energy balance

$$\varepsilon_s \left(\rho C_p\right)_s \frac{\partial T_s}{\partial t} = \frac{\partial}{\partial x}\left(\lambda_s^* \frac{\partial T_s}{\partial x}\right) + \Gamma_{g,s}\left(T_s - T_g\right) + Q_g + h\left(T_{amb} - T_s\right) \tag{17}$$

4. Perfect Gas Law

$$\rho_g = \frac{P_g M_g}{R T_g} \tag{18}$$

4.2.4 Numerical Integration

A standard sequential non-iterative operator splitting scheme was used to solve the resulting non-linear problem. Firstly is solved the mass and energy transports term, thanks to a transport operator which uses a full sequential approach and finite volume schemes (Lapene, 2006). Finally, the chemistry operator, which is reduced to a stiff ODE system, is solved by the LSODES FORTRAN library, which uses backward differentiation formulas by Gear, (Hindmarsh, A. C., Radhakrishnan, K., 1993).

Figure 3, shows schematically the reactor combustion used in the numerical simulation. A general nodal point is identified by P and its neighbors in a one-dimensional geometry. The north side face of the control volume is referred by 'N' and the south side control volume face by 'S'. The nodes to the northeast and southeast, are identified by 'n' and 's', respectively.

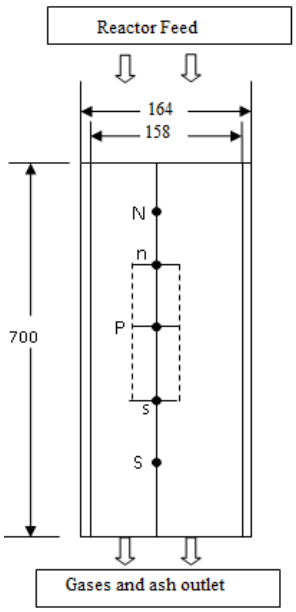

Figure 3. Reactor combustion used in the numerical simulation scheme. Adapted from Versteeg, H.K., Malalasekera, W., 2007.

The input data for the program are described in the table below:

Table 1. Values of parameters used in the model for pellets combustion.

Ambient Temperature	300 K
Atmospheric pressure	1.013×10^5 Pa
Reactor length	700 mm
Number of nodes	700
Time step	0.005 s
Time of experiment	33000 s
Density of the pellets	973 Kg/m³
Air inlet velocity	0.00101 m/s
Porosity of the bed	0.51
Thermal diffusivity	1.0×10^{-6} m^2/s
Permeability	2.55×10^{-14} m^2
Specific surface of solid fuel	3600 m^{-1}
Pellets diameter	9.51×10^{-3} m
Initial mass fraction of solid fuel	0.3100
Mass fraction of inert matter	0.6550
Initial mass fraction of water	0.03500

5 EXPERIMENTAL RESULTS AND NUMERICAL ANALYSIS

Comparative analysis between the experimental and numerical result is done considering the Fig. 4. It can be observed for numerical and experimental results that the temperature increase rate have a good agreement at largely of the time. After the combustion front reaches the maximum value in thermocouples 1, 2, 3, 4, 5, 6 and 7, the temperature drop is slower for the experimental result. An explanation for the differences in temperature decreases between the experimental and numerical results happen is that in the experimental results, into combustion reactor, after the front reaches a maximum value, the temperatures remain high due to the remaining heat of the combustion front. It can be seen that the peak temperatures results for the experiment and for numerical method has a good agreement.

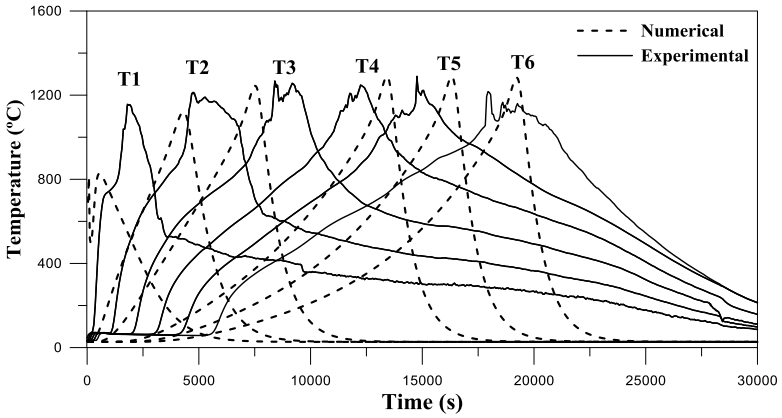

Figure 4 - Evolution of numerical and experimental temperatures.

It is observed to the experimental result that near of the maximum temperature region an instability of the temperature. This instability can be attributed to the effect of accommodating of the fuel pellets while the charcoal is consumed during the combustion. The numerical result can't show such instabilities observed in the experimental result as show Fig. 4. The implementation of a reaction into the model makes necessary for detect such instability and improve it.

From the maximum temperature point where there was a accommodation of the fuel, the structure of the bed becomes more stable and the temperature evolution becomes smoother. After completion of the reaction the temperature decreases rapidly, showing that there is little heat generation after the forward reaction has been completed. The maximum temperature remains practically constant throughout the bed and decreases significantly only when the forward reaction consumes the whole fuel.

The difference of temperature between experimental and numerical results to thermocouple 1, it is because to realization of this work, the combustion reactor it was completely filled with pellets, and the distance of the top of reactor, where starts the ignition, to termocouple 1, is 50 mm, what provoke the discrepancy in temperature, observe the Fig. (1a), Fig. (1b) and Fig. 2.

For thermocouple 7, it was observed "in loco" that there was a great discrepancy between the numerical and the experimental temperatures results shown in Fig. (5b). The accumulation of materials on the bottom of the combustionn reactor and over the thermocouple sensor could act as a thermal insulator as shows Fig.(5a), keeping the temperature around 800 ° C during about 6000 seconds, then the temperature begins to fall. Parameters as porosity, diffusivity, specific mass, the reaction velocity and ignition timing were set, as shown in Tab. 1, for geting the numerical result shown in Fig. 4 and Fig.(5b).

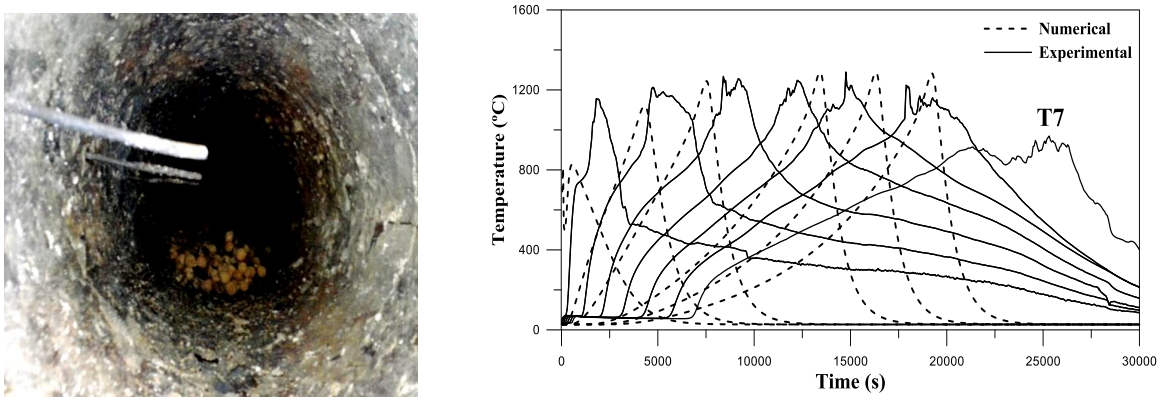

(a) (b)

Figure 5 - (a) Accumulated pellets on bottom of combustion reactor ; (b) Thermocouple 7, front combustion analysis

6 CONCLUSION

The computer code used for validation of experimental results, presents a result enough consistent with the experiments results in the combustion reactor before the combustion reaction reaches the peak temperature, however after the combustion front reaches the peak temperature and start to decrease, it is observed that there is a very intense discrepancy between numerical result and the experimental result.

The difference of temperature between experimental and numerical results detected by thermocouple 1, it is in consequence of distance of that thermocouple to the top of the reactor completaly filled with pelllets.

Thermocouple 7, shows a great discrepancy between the numerical temperatures and the experimental temperatures results in consequence of accumulation of materials on the thermocouple sensor that could act as a thermal insulator, keeping the temperature around 800°C during about 6000 seconds. On the other hand the maximum temperatures registered by thermocouples 2, 3, 5 and 6 are practically equal with the numerical result.

It's also concludes that the computer code can' t detect instabilities presented in the experiment at the point of maximum temperatures due to accommodation of the pellets during the combustion reaction then implementation of a reaction into the model makes necessary for detect such instability and improve it.

ACKNOWLEDGEMENTS

The authors are thankful to CAPES, FAPEMA, IFMA and PRODERNA-UFPA for their respective research support.

REFERENCES

Bejan, Adrian., A. Nield., Donald., 2006. *Convection in Porous Media,* Fourth Edition, New York, Springer.

Hindmarsh, A. C., Radhakrishnan, K., 1993. Description and Use of LSODE, the Livermore Solver for Ordinary Differential Equations. NASA Ref. Publ. 1327, Report UCRL-ID-113855. Lawrence Livermore National Laboratory, Livermore, CA.

Kaviany, M., 1995. *Principles of Heat Transfer in Porous Media*, Second Edition, Springer-Verlag New York, Inc., New York. Check 1995 second edition.

Lapene, A., 2006. *Modelisation numerique de la combustion en lit fixe de combustibles solides.* Rapport de stage, IMFT, Toulouse: Master Recherche en Dynamique des Fluides, Energetique et Transferts.

Lapene, A., G. Debenest, M. Quintard, M. F. Martins, S. Salvador., 2008. "Numerical Simulation of Combustion in Reactive Porous Media." *International Review of Mechanical Engineering (I.RE.M.E.)*.

Versteeg, H.K., Malalasekera, W., 2007. *An Introduction to Computational Fluid Dynamics.* The Finite Volume Method. Second Edition. Pearson Prentice Hall.

Martins, M.F., 2008. "*The structure of a combustion front propagating in a fixed bed of crushed oil shale:co-current configuration*", These-Doctorat de L' Université de TOULOUSE.

Whitaker, S., O. Plumb., 1988. Dispersion in heterogeneous porous media: Local volume averaging and large-scale averaging. Latin American Applied Research 18: 71-79.

X. Zou., J. L, Torero., Bregon, B., 1995. On the Propagation of a Reaction Front Through a Porous Fuel in the Presence of an Opposed Forced Flow: Application to Mixtures Characteristic of Municipal Waste. Université de Poitiers - UPR.